Modelling thermo-hygro-mechanical behaviour of High Performance Concrete in high temperature environments

D.Gawin
Department of Building Physics and Building Materials, Technical University of Lodz, Lodz, Poland

C.E.Majorana, F.Pesavento & B.A.Schrefler
Department of Structural and Transportation Engineering, University of Padova, Padova, Italy

ABSTRACT: The present work deals with an innovative model for analyzing the behaviour of concrete in high temperatures conditions. In particular it is focused on High Performance and Ultra High Performance concretes which have been often used in the last decade in nuclear engineering applications, tall buildings and in tunnels. In such cases prediction of concrete performance during and after fire exposure is of great practical importance, in particular as far as tunnels are concerned, as recent fires in major European tunnels have demonstrated. Nowadays, it is well established that phenomena which take place in concrete exposed to high temperatures, cannot be studied by means of purely diffusive models. In the model presented in this paper concrete is treated as partially saturated porous material and allows to consider hydration-dehydration, evaporation-condensation, adsorption-desorption phenomena and non-linearities due to temperature and pressure. An application of this model to an HP concrete structure will be shown.

1 INTRODUCTION

1.1 General overview of concrete at high temperature

When concrete is exposed to high temperature a rather complex analysis is required to deal with the coupled heat and mass transfer that can occur, involving both liquid mass transfer and vapour mass transfer and related mechanical effects (Bazant & Kaplan, 1996).

In such severe conditions in terms of temperatures and pressures, assessment of concrete performance is of great interest in nuclear engineering applications, in safety evaluation in tall buildings and in tunnels (Bazant & Thonguthai, 1978,1979). In particular as far as tunnels are concerned, recent major fires in key European tunnels (Channel, Mont-Blanc, Great Belt Link, Tauern) emphasised the serious hazards they present in human and economic terms. In these accidents, in the affected sections, tunnels presented extensive damage to the concrete elements. Part of the concrete lining was almost completely removed by spalling.

Spalling, which may be explosive, is mainly due to different coexisting coupled processes, such as thermal (heat transfer), chemical (dehydration of cement paste), hygral (transfer of water mass, in liquid and vapour form) and mechanical processes.

In general, moisture transport may include air-vapour mixture flow due to forced convection, free convection, and infiltration through cracks and pores, vapour transport by diffusion, flow of liquid water due to diffusion, capillary action, or gravity, and further complications associated with phase changes due to condensation/evaporation, freezing/thawing, ablimation/sublimation, and adsorption/desorption.

Movement of air and water through the concrete is accompanied by significant energy transfer, associated with the latent heat of water and the heats of hydration and dehydration. At temperature largely above critical point of water important chemical transformations of components of concrete take place.

These situations are much more dangerous in the case of High Performance and Ultra High Performance concrete. At ambient temperature, in fact, these kinds of concrete present much better features than a normal concrete because of their lower permeability, lower porosity and higher compactness. This means greater mechanical strength, in particular as far as the compression strength is concerned, and an improved durability. At low temperatures, in fact, the cement matrix increases the strength of high performance concrete, because of its higher density and homogeneity, involving a better distribution of the stresses than a traditional concrete. At higher temperature this matrix becomes the weak point of the materials showing low mechanical strength. With the temperature increase the aggregates progressively expand as long as they are not chemically altered, while the cement matrix, after an initial ex-

pansion, is subject (over 150°C) to a progressive shrinkage. These two opposite phenomena involve a micro-cracking process which involve damaging of the material microstructure. Further, low permeability inhibits water mass transfer causing high gas pressure values, crack-opening and then an increase of intrinsic permeability.

Hence, for concrete, particularly at high temperature, one cannot predict heat transfer only from the traditional thermal properties: thermal conductivity and volumetric specific heat. Similarly, it is not possible to predict mass transfer considering this phenomenon as purely diffusive.

2 MATHEMATICAL MODEL

2.1 Introduction

In the model presented here, concrete is considered as a partially saturated porous material (Gawin & Schrefler, 1996) consisting of a solid phase, two gas phases and three water phases. The theoretical framework is based on the works of Whitaker (1977), Bear (1988), Bear & Bachmat (1986, 1889), Hassanizadeh and Gray (1979, 1980) and Lewis & Schrefler (1998).

Refinements such as non-linearities due to temperature and pressures, hydration-dehydration, evaporation-condensation, adsorption-desorpion, phenomena are considered, (Gawin et al., 1998, Gawin et al., 1999). Different physical mechanisms governing the liquid and gas transport in the pores of partially saturated concrete are clearly distinguished, i.e. capillary water and gas flows driven by their pressure gradients, adsorbed water surface diffusion caused by saturation gradients, as well as air and vapour diffusion driven by vapour density gradients, (Gawin et al., 1998, 1999). Concrete damaging effects arising from coupled hygro-thermal and mechanical interaction are considered by use of the isotropic non-local damage theory and a further coupling between intrinsic permeability and mechanical damage has been introduced to take into account the changes of material microstructure. Moreover improvements, regarding the possibility to simulate the behaviour of the material at temperatures which largely exceed the critical point of water and the real behaviour of gases present in the pores of concrete, i.e. the gases are treated as real gas, have been recently introduced in the model (Gawin et al., in prep.).

2.2 Governing equations

The final mathematical model consists of four balance equations: mass conservation of dry air, mass conservation of the water species (both in liquid and gaseous state, taking phase changes, i.e. evaporation - condensation, adsorption - desorption and hydra-

tion - dehydration process, into account), enthalpy conservation of the whole medium (latent heat of phase changes and heat effects of hydration or dehydration processes are considered) and linear momentum of the multiphase system. They are completed by an appropriate set of constitutive and state equations, as well as some thermodynamic relationships, (Lewis & Schrefler, 1998). The governing equations of the model are expressed in terms of the chosen state variables: gas pressure p^g, capillary pressure p^c, temperature T and displacement vector of the solid matrix $\mathbf{u}$ and are directly derived from Lewis & Schrefler (1998), where the constitutive law for the solid skeleton density and water density are experimentally determined. In particular the density of solid skeleton has to respect the solid mass conservation equation which is not a basic equation of the model. The governing equations of the model proposed, considering negligible both the inertial forces and the convective heat flux related to solid phase and taking into account the Bishop's stresses (Schrefler & Gawin, 1996), are the following:

Dry air mass conservation equation:

$$
-\,n\frac{\partial S_w}{\partial t} - \beta_s\left(1-n\right)S_g\frac{\partial T}{\partial t} + S_g\nabla\cdot\mathbf{v}^s +
$$
$$
+\frac{S_g n}{\rho^a}\,\frac{\partial \rho^a}{\partial t} + \frac{1}{\rho^a}\nabla\cdot\mathbf{J}_g^a +
$$
$$
+\frac{1}{\rho^a}\nabla\cdot\left(nS_g\rho^a\mathbf{v}^{gs}\right) + \tag{1}
$$
$$
+\frac{\left(1-n\right)S_g}{\rho^s}\,\frac{\partial \rho^s}{\partial \Gamma_{hydr}}\frac{\partial \Gamma_{hydr}}{\partial t} = \frac{\dot{m}_{dchydr}}{\rho^s}S_g
$$

Water species (liquid + vapour) mass conservation equation:

$$
n\left(\rho^w - \rho^v\right)\,\frac{\partial S_w}{\partial t} - \beta_{swg}\frac{\partial T}{\partial t} +
$$
$$
+\left(\rho^v S_g + \rho^w S_w\right)\nabla\cdot\mathbf{v}^s + S_g n\,\frac{\partial \rho^v}{\partial t} +
$$
$$
+\nabla\cdot\mathbf{J}_g^v + \nabla\cdot\left(nS_g\rho^v\mathbf{v}^{gs}\right) + \nabla\cdot\left(nS_w\rho^w\mathbf{v}^{ws}\right) + \tag{2}
$$
$$
+\frac{\left(1-n\right)\left(S_g\rho^v + \rho^w S_w\right)}{\rho^s}\,\frac{\partial \rho^s}{\partial \Gamma_{hydr}}\frac{\partial \Gamma_{hydr}}{\partial t} =
$$
$$
=\frac{\rho^v S_g + \rho^w S_w - \rho^s}{\rho^s}\dot{m}_{dchydr}
$$

Energy conservation equation (enthalpy balance):

$$
\left(\rho C_p\right)_{cf}\frac{\partial T}{\partial t} + \left(\rho_w C_p^w\mathbf{v}^{ws} + \rho_g C_p^g\,\mathbf{v}^{gs}\right)\cdot\nabla T -
$$
$$
-\nabla\cdot\left(\lambda_{cf}\nabla T\right) = \tag{3}
$$
$$
=-\dot{m}_{phase}\,\Delta H_{phase} + \dot{m}_{dchydr}\Delta H_{dchydr}
$$

Linear momentum equation (equilibrium equation):

$$div\left\{\sigma' - \mathbf{I}(p^g - S_w p^c)\right\} + \rho\mathbf{g} = 0 \qquad (4)$$

For the closure of the model a set of thermodynamic and constitutive relationships are needed. In the present work only few of them will be shown in detail, in particular as far as damage mechanics and absolute permeability-damage parameter coupling are concerned. For further information see Gawin et al. (1998), Gawin et al. (1999), Schrefler & Gawin (1996) and Lewis & Schrefler (1998).

2.3 Thermodynamic and constitutive relationships

2.3.1 Dehydration law

As above mentioned, dehydration processes, involving cement gel and carbon idroxide, are of importance. In order to describe the heat sinks and the skeleton mass sinks related to these chemical reactions, it is necessary to know the time evolution of degree of cement hydration $\Gamma_{hydr}(t)$. It may be described by a formula of the following form:

$$\Gamma_{dchydr}(t) = \Gamma_{dchydr}[T_{\max}(t)] \qquad (5)$$

where $T_{\max}(t)$ is the highest temperature reached by the concrete up to the time instant t.

The dehydrated water content $\Delta m_{hydr}(T)$ increases, when temperature increases, approximately following a step function showing a sharp change between 200°C and 500 °C. Such a kind of behaviour can be represented from the following law:

$$\Delta m_{dchydr} = f_s\, m\, c\, f(T) \qquad (6)$$

where f_s is stechiometric factor, m is ageing degree of concrete (between 0 and 1), c is the cement content and $f(T)$ is an function of temperature.
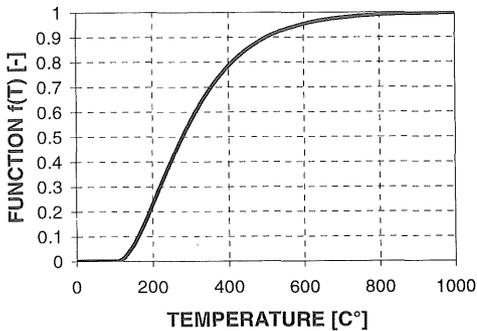
Figure 1. Function of dehydration $f(T)$ for an ordinary concrete according to equation (6)

2.3.2 Water vapour density

Water vapour is treated as real gas, hence its mass density can be expressed in the form (in saturated conditions):

$$\rho^v = \rho^v(T, p^v) = \left[p^v\frac{M_w}{RT} + \Delta\rho^v\right] \qquad (7)$$

Where the first term at right hand side of eq. (7) corresponds to the Clapeyron law, while the second one represents the deviation from an ideal behaviour.

Figure 2 represents the differences between ideal and real behaviour:
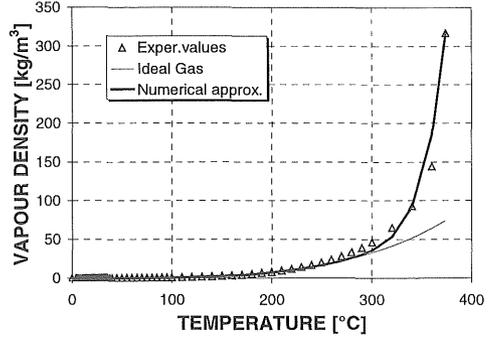
Figure 2. Vapour density as function of temperature: ideal and real behaviour according to equation (7)

2.4 Damage mechanics

The concrete damage at high temperature (cracks development) is considered, following the model of scalar isotropic damage by Mazars (1984) and Mazars & Pijaudier-Cabot (1989). In this model, the material is supposed to behave elastically and to remain isotropic, and it is assumed that only the elastic properties of the material are affected by damage. A "modified effective stress" σ taking into account the damage D ($0 \leq D \leq 1$) as a parameter measuring the reduction of resistant area due to crack beginning and spreading, is introduced. Hence, the stress tensor σ and the damage energy released rate Y are as follows:

$$\sigma = \Lambda_0(1 - D) : \varepsilon^e \;;\; Y = \frac{1}{2}\Lambda_0 : \varepsilon^e : \varepsilon^e \qquad (8)$$

where Λ_0 is the initial stiffness matrix of the material and ε^e is the elastic part of strains.

The effective stress concept leads to the following form of the elastic energy (Mazars, 1984, 1986):

$$\rho\psi_c = \frac{1}{2}\Lambda_0(1 - D) : \varepsilon^e : \varepsilon^e \qquad (9)$$

where $\rho\psi_c$ is a scalar thermodynamic potential (ρ is the density of the material).

Taking into account different performance of

concrete in traction and in compression, i.e. coupling of two types of damage D_t and D_c (Mazars, 1984), the final expression for the stress has the following form:

$$\sigma_i = \left\{ (1 - A_i) K_0 + \frac{A_i \varepsilon}{\exp\left[B_i (\varepsilon - K_0) \right]} \right\} E \qquad (10)$$

where $i=t,c$. The parameters A_t, A_c, B_t, B_c are characteristics of the material and temperature dependent. K_0 is the initial value of the hardening/softening parameter $K(D)$, which satisfies the principle of maximum de Saint-Venant's strain (loading function)

$$f(\varepsilon, \Lambda, K_0) = \tilde{\varepsilon} - K(D) \qquad (11)$$

where the equivalent strain $\tilde{\varepsilon}$ is defined as follows

$$\tilde{\varepsilon} = \sqrt{\sum (\langle \varepsilon_i \rangle_+)^2} \; ; \; \left(\langle x \rangle_+ = \frac{|x| + x}{2} \right) \qquad (12)$$

ε_i being the principal strains.

2.5 Damage-intrinsic permeability coupling

A phenomenological approach is usually applied for description of changes of concrete physical properties during complex hygro- thermal and mechanical phenomena at high temperature. It means that all these changes are expressed as a function of temperature, moisture content and gas pressure, i.e. physical quantities measured directly during experimental tests. However results of such tests are strongly dependent upon the form and dimensions of a test sample, as well as physical conditions during experiment. Hence application of the results of these tests for prediction of concrete behaviour in conditions that differ significantly from the experimental ones is rather questionable.

Because of this there is a need for mechanistic (structural) mathematical models which assume certain physical models of the phenomena analysed. Significant increase of concrete intrinsic permeability at high temperature is mainly generated by arising micro-cracks and by changes of material inner structure, as well as by crack-opening due to high gas pressure values. As a result, it depends not only upon temperature, moisture content and gas pressure, as assumed for a phenomenological approach, but also upon a degree of cracks development, which may be described by use of damage parameter D.

There is still lack of sufficient experimental research to form a basis of a mathematical model of these complex phenomena. However one can expect that a joint effect of temperature, gas pressure and material damaging (crack development) on the intrinsic material permeability, k, may be described by:

$$k = k_0 \cdot 10^{A_T(T - T_n)} \cdot \left(\frac{p_g}{p_0} \right)^{A_p} \cdot 10^{A_D D} \qquad (13)$$

where A_T, A_P and A_D are material constants.

Parameter A_P in (13) has a clear physical interpretation, because it describes effect on the material permeability increase of crack opening caused by pressure rise. The parameter A_D in (13) is dependent on the type and dimensions of the cracks developed in concrete matrix, (Gawin et al., 1998).

3 NUMERICAL MODEL

The system of governing equations of the model (1)-(4), after application of the finite element method for discretization in space and backward finite difference scheme for temporal derivatives, similarly as in Gawin et al. (1999), may be written in the following concise form:

$$\frac{1}{\Delta t} \left[\frac{\partial}{\partial \mathbf{x}} \mathbf{C}\left(\mathbf{x}_{n+1}^l\right)\left(\mathbf{x}_{n+1}^l - \mathbf{x}_n\right) + \atop \mathbf{C}\left(\mathbf{x}_{n+1}^l\right) \right] \Delta \mathbf{x}_{n+1}^l +$$

$$\left[\frac{\partial}{\partial \mathbf{x}} \mathbf{K}\left(\mathbf{x}_{n+1}^l\right) \mathbf{x}_{n+1}^l + \atop \mathbf{K}\left(\mathbf{x}_{n+1}^l\right) + \frac{\partial}{\partial \mathbf{x}} \mathbf{f}\left(\mathbf{x}_{n+1}^l\right) \right] \Delta \mathbf{x}_{n+1}^l = \qquad (14)$$

$$= - \left[\mathbf{C}\left(\mathbf{x}_{n+1}^l\right) \frac{\mathbf{x}_{n+1}^l - \mathbf{x}_n}{\Delta t} + \atop \mathbf{K}\left(\mathbf{x}_{n+1}^l\right) \mathbf{x}_{n+1}^l + \mathbf{f}\left(\mathbf{x}_{n+1}^l\right) \right]$$

with:

$$\mathbf{K}_{ij} = \begin{bmatrix} \mathbf{K}_{gg} & \mathbf{K}_{gc} & \mathbf{K}_{gt} & \mathbf{0} \\ \mathbf{K}_{cg} & \mathbf{K}_{cc} & \mathbf{K}_{ct} & \mathbf{0} \\ \mathbf{K}_{tg} & \mathbf{K}_{tc} & \mathbf{K}_{tt} & \mathbf{0} \\ \mathbf{K}_{ug} & \mathbf{K}_{uc} & \mathbf{K}_{ut} & \mathbf{K}_{uu} \end{bmatrix} \qquad (15a)$$

$$\mathbf{C}_{ij} = \begin{bmatrix} \mathbf{C}_{gg} & \mathbf{C}_{gc} & \mathbf{C}_{gt} & \mathbf{C}_{gu} \\ \mathbf{0} & \mathbf{C}_{cc} & \mathbf{C}_{ct} & \mathbf{C}_{cu} \\ \mathbf{0} & \mathbf{C}_{tc} & \mathbf{C}_{tt} & \mathbf{C}_{tu} \\ \mathbf{0} & \mathbf{0} & \mathbf{0} & \mathbf{0} \end{bmatrix} \quad \mathbf{f}_i = \begin{Bmatrix} \mathbf{f}_g \\ \mathbf{f}_c \\ \mathbf{f}_t \\ \mathbf{f}_u \end{Bmatrix} \qquad (15b)$$

4 NUMERICAL EXAMPLE

This example deals with a I beam subjected to fire. Considering the shape of the sample, a quarter of the cross section of the beam has been discretized by 173 eight node serendipity elements, see Figure 3. Initial values of relative humidity equal to 50% and temperature equal to 298.15 K are assumed. On the external surface mixed, convective and radiative, BCs for energy exchange, with heat exchange coefficient $\alpha_c = 18$ W/m^{2}K, surface emmisivity $e\sigma_o =$

$5.1 \cdot 10^{-8}$ W/(m²K⁴) and ambient temperature increases following the standard ISO fire curve, are considered. For mass exchange convective BCs with p_v=1000 Pa and mass exchange coefficient β_c= 0.018 m/s are assumed.

The analysed material is High Performance Concrete of the class 80 MPa compressive strength and it is characterised by the following parameters (at initial state):

1. dry state apparent density - ρ_o= 2590 kg/m³,
2. initial porosity - Φ=0.12,
3. initial thermal conductivity of dry material - λ_{dry}= 1.5 W/(m·K),
4. initial intrinsic permeability - K_o= 10^{-21} m²,
5. compressive strength, f_c= 80 MPa,
6. Young's modulus E= 44 GPa and Poisson's ratio v=0.20.
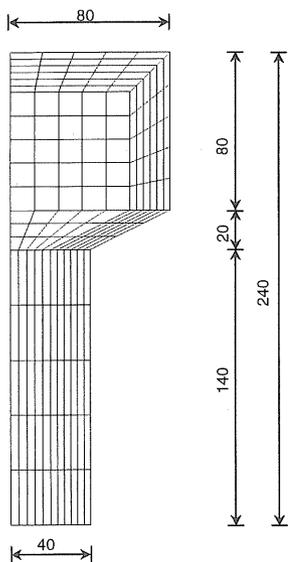
Figure 3. Geometry and discretization of cross section of the beam

The problem has been solved using the damage-intrinsic permeability coupling according to Eqn. 13. In the Figure 4a and b, the dependence of compressive and tensile strength on temperature are shown.

They were extrapolated from experimental data measured during the European research program BRITE Euram III "Hiteco" (1999).

These curves have been used for determining the coefficients A_c, B_c, A_t, and B_t needed for Mazar's law. Similarly hygro-thermal and microstructural properties of this material have been used from the above mentioned European research project. In Figure 4c thermal conductivity of solid and porosity of concrete are shown as example.

At the beginning of the simulation, after 2 minutes, only the surface layer and the zone close to the corner are subjected to an increase of temperature and a desaturation process due to external heating, (Fig. 5 a and b). In the relative humidity distribution map the thermo-diffusion phenomenon is already visible at this time causing a rise of RH values inside the beam (Fig. 5b). The damage, stresses and vapour pressure do not reach significant values.

a)

b)

c)
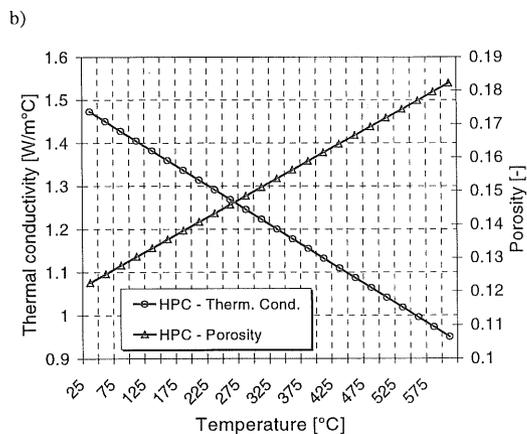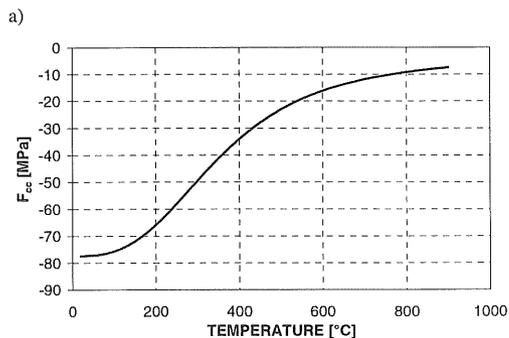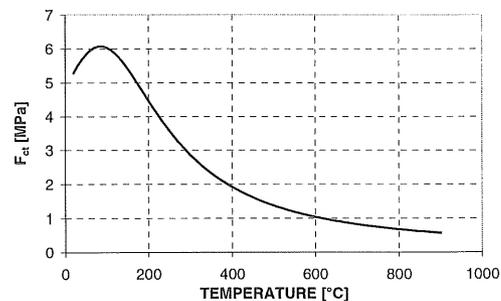
Figure 4. Compressive strength a), tensile strength b), and thermal conductivity and porosity c), of concrete used in the calculation

After 10 minutes a larger part of the section is subjected to the desaturation process and the thermal

203

front is interesting the core of the beam, (Fig. 6 *a,b*), while the temperature in the corner has passed the critical point of water.

a)   b)

Figure 5. Temperature (a) and relative humidity distribution (b) at 2 minutes

As above mentioned these physical, chemical and mechanical processes, involving a reduction of Young's modulus, a decrease of final strength and a different slope in the softening part of stress-strain curve, lead to a progressive damaging of concrete and may result in a collapse of the structure and/or spalling (Fig. 6*a*). At 10 minutes the damaged zone is extended on whole external side of the beam. Vapour pressure peak, around 2 MPa (Fig. 6*d*), is located close to the corner and, considering damage distribution, a spalling occurrence interesting the zone near the corner of the cross section it is possible.

5 CONCLUSIONS

A finite element model of concrete at high temperature based on a mechanistic approach has been presented. Concrete is considered as multiphase porous material in which adsorption-desorption, hydration-dehydration, evaporation-condensation, different fluid flows and non-linearities with temperature have been taken into account. The particular approach permits to consider the different phenomena, which

take place in concrete during heating and their coupling.

a)   b)

c)   d)
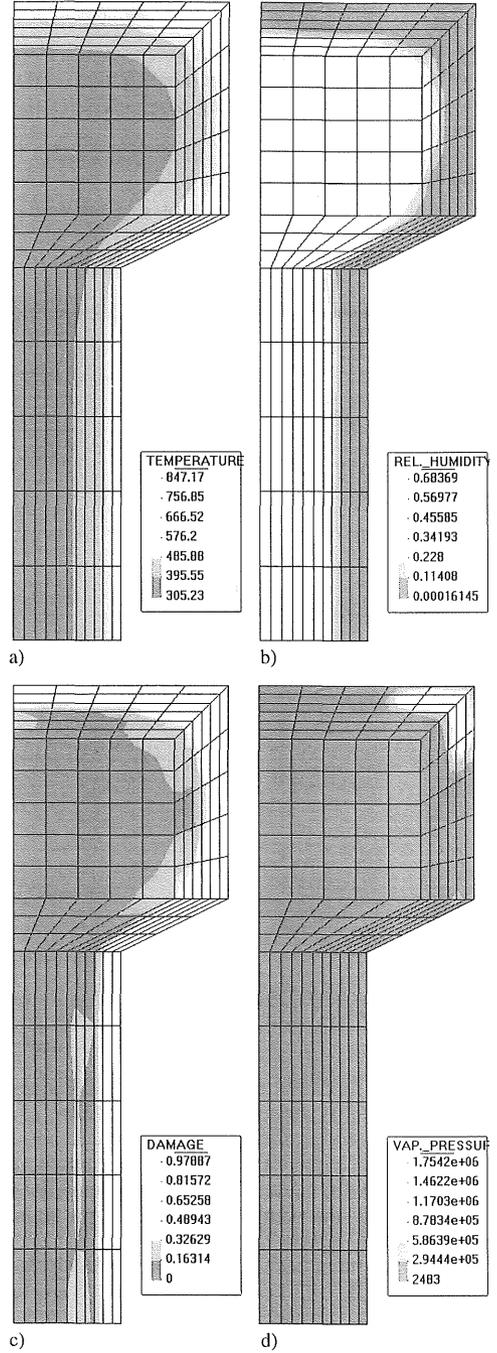
Figure 6. Temperature (a), relative humidity (b), damage (c) and vapour pressure (d) at 10 minutes

The resulting model is appealing for prediction of thermo-hygro-mechanical behaviour of concrete structures in such severe conditions as shown with a 2D example. Phenomena concerning real behaviour of gases close to critical point of water, behaviour of concrete in a range of temperature largely above 374.15 °C, and saturation plug process, have been recently investigated and introduced in the model.

ACKNOLEDGEMENTS

NOMENCLATURE

C_p effective specific heat of porous medium [J kg^{-1} K^{-1}]
C_p^g specific heat of gas mixture [J kg^{-1} K^{-1}]
C_p^w specific heat of liquid phase [J kg^{-1} K^{-1}]
D   damage parameter
D_{eff} effective diffusion of gas mixture [m^2 s^{-1}]
e emmisivity of the interface [-],
E   Young's modulus [Pa]
F_{cc} compressive strength of concrete [MPa]
F_{ct} tensile strength of concrete [MPa]
g   gravity acceleration [m/s^2]
I   unit tensor
$\mathbf{J}_g^v$ diffusive flux of vapour
$\mathbf{J}_g^a$ diffusive flux of dry air
k   absolute permeability [m^2]
k^{rg} relative permeability of gas phase [-]
k^{rl} relative permeability of liquid phase [-]
M_w molar mass of water vapour [kg kmol^{-1}]
$\dot{m}_{phase}$ rate of mass due to phase change [kg m^{-3} s^{-1}]
$\dot{m}_{dehydr}$ rate of mass due to dehydration [kg m^{-3} s^{-1}]
n   total porosity (pore volume/total volume) [-]
p^c capillary pressure [Pa]
p^g pressure of gas phase [Pa]
p^v water vapour partial pressure [Pa]
p^{vs} water vapour saturation pressure [Pa]
R   gas constant (8314.41 J kmol^{-1} K^{-1})
S_w liquid phase volumetric saturation (liquid volume/pore volume) [-]
S_g gas phase volumetric saturation (liquid volume/pore volume) [-]
t time [s]
T temperature [K]
T_{cr} critical temperature of water [K]
u   displacement vector of solid matrix [m]
$\mathbf{v}^{gs}$ relative velocity of gaseous phase [m s^{-1}]
$\mathbf{v}^{ws}$ relative velocity of liquid phase [m s^{-1}]
$\mathbf{v}^s$ velocity of solid phase [m s^{-1}]

α_c convective heat transfer coefficient [W m^{-2} K^{-1}]
β_c convective mass transfer coefficient [m s^{-1}]
β_s cubic thermal expansion coefficient of solid [K^{-1}]
β_{swg} combine cubic thermal expansion coefficient [K^{-1}]
ΔH_{vap} enthalpy of vaporization per unit mass [J kg^{-1}]
ΔH_{dehydr} enthalpy of dehydration per unit mass [J kg^{-1}]
Δm_{dehydr} mass source term related to hydration-dehydration process [kg m^{-3}]
Δt time step [s]
ε strains tensor [-]
ε^e elastic strain tensor [-]
Γ_{hydr} degree of hydration (or dehydration) [-]
Λ_o initial stiffness matrix
λ_{ef} effective thermal conductivity [W m^{-1} K^{-1}]
ν Poisson's ratio [-]
ρ apparent density of porous medium [kg m^{-3}]
ρ^g gas phase density [kg m^{-3}]
ρ^w liquid phase density [kg m^{-3}]
ρ^s solid phase density [kg m^{-3}]
ρ^a mass concentration of dry air in gas phase [kg m^{-3}]
ρ^v mass concentration of water vapour in gas phase [kg m^{-3}]
σ,   Cauchy stress tensor [Pa]
σ' Effective stress tensor [Pa]
σ_o Stefan-Boltzmann constant [W m^{-2} K^{-1}]

REFERENCES

Bazant, Z.P. & Thonguthai, W. 1978. Pore pressure and drying of concrete at high temperature. In J. Engng. Mech. Div. ASCE. 104,: 1059-1079.

Bazant, Z.P. & Thonguthai, W. 1979. Pore pressure in heated concrete walls: theoretical prediction. In Mag. of Concr. Res. 31(107): 67-76.

Bazant, Z.P. & Kaplan, M.F. 1996. Concrete at High Temperatures: Material Properties and Mathematical Models. Harlow: Longman,.

Bear, J. 1988. Dynamics of fluids in porous media. New York: Dover.

Bear, J. & Bachmat, Y. 1986. Macroscopic modelling of transport phenomena in porous media, 2: applications to mass momentum and energy transfer. In Transp. in Porous Media 1: 241-269.

Bear, J. & Bachmat, Y. 1990. Introduction to modelling of transport phenomena in porous media. Dordrecht: Kluwer,.

Brite Euram III BRPR-CT95-0065 1999 "HITECO". Understanding and industrial application of High Performance Concrete in High Temperature Environment. Final Report.

Gawin, D. & Schrefler, B.A. 1996. Thermo- hydro- mechanical analysis of partially saturated porous materials. In Engineering Computations 13(7): 113-143.

Gawin, D., Majorana, C.E., Pesavento, F., & Schrefler, B.A 1998. A fully coupled multiphase FE model of hygro-thermo- mechanical behaviour of concrete at high temperature. In Computational Mechanics., Onate, E. & Idelsohn, S.R. (eds.), New Trends and Applications:, Proc. of the 4th World Congress on Computational Mechanics, Buenos Aires 1998: 1-19. Barcelona: CIMNE.

Gawin, D., Majorana, C.E., Schrefler, B.A. 1999. Numerical analysis of hygro-thermic behaviour and damage of concrete at high temperature. In Mech. Cohes.-Frict. Mater. 4: 37-74.

Gawin, D., Pesavento, F., & Schrefler, B.A. Modelling of hygro-thermal behaviour and damage of concrete at temperature above the critical point of water. in prep..

Hassanizadeh, M. & Gray, W.G. 1979. General conservation equations for multiphase systems: 1. Averaging technique. In Adv. Water Res. 2: 131-144.

Hassanizadeh, M. & Gray, W.G. 1979. General conservation equations for multiphase systems: 2 Mass, momenta, energy and entropy equations. In Adv. Water Res. 2: 191-203.

Hassanizadeh, M. & Gray, W.G. 1980. General conservation equations for multiphase systems: 3 Constitutive Theory for Porous Media. In Adv. Water Res. 3: 25-40.

Lewis, R.W., & Schrefler, B.A. 1998. The Finite Element Method in the Static and Dynamic Deformation and Consolidation of Porous Media. Chichester: Wiley & Sons.

Mazars J. 1984. Application de la mecanique de l' endommagement au comportament non lineaire et la rupture du beton de structure (in French). Thesy de Doctorat d' Etat, L.M.T., Universite de Paris.

Mazars, J. 1986. Description of the behaviour of composite concretes under complex loadings through continuum damage mechanics. In Lamb, J.P. (ed.); Proc. of the 10th U.S. National Congress of Applied Mechanics. ASME.

Mazars, J. & Pijaudier-Cabot, J. 1989. Continuum damage theory - application to concrete. In J. of Eng. Mechanics ASCE 115(2): 345-365.

Schrefler, B.A. &, Gawin, D. 1996. The effective stress principle: incremental or finite form?. In Int. J. for Num. and Anal. Meth. in Geomechanics 20(11): 785-815.

Whitaker, S. 1977. Simultaneous heat mass and momentum transfer in porous media: a theory of drying. In Advances in heat transfer 13. New York: Accademic Press.